

# Nanovortex evolution in entrance part of the 2D open type long nanocavity

A. KORDOS\* and A. KUCABA-PIETAL

Rzeszow University of Technology, Faculty of Mechanical Engineering and Aeronautics, Powstancow Warszawy 8 Av., 35-959 Rzeszow, Poland

**Abstract.** Non-equilibrium molecular dynamics method (NEMD) is applied to investigate a formation process of water nanovortex in 7 nm wide nanocavity (aspect ratio of which was equal to 3.6). The flow in the nanocavity was induced by Poiseuille 2D water nanoflow in a main nanochannel, to which the nanocavity is situated perpendicularly. The wall of main channel and the nanocavity is made from quartz. Flow is induced by applying constant force to molecules inside the main channel. Based on NEMD simulation data, the sequence of images representing water velocity vector fields was obtained at constant time intervals equal to 1 ns, which shows vortex formation mechanism. Flow field images analysis indicates that the shape and centre position of the nanovortex vary slightly each nanosecond, nevertheless, the structure remains stable in the flow field at the entrance to the nanocavity.

**Key words:** nanofluidics, molecular dynamics, nanocavity, nanovortices, nanodevices.

## 1. Introduction

Control of microscale and nanoscale fluid flows has become an important research theme in micro- and nano-technology. Interest in the use of microcavity vortices in miniaturized devices caused a growth of research on flows through microchannels with microcavities in the last decade [25, 27, 32]. Its results caused that currently microvortices in microcavity are the basis of operation of many bio-micro-devices, such as: microcentrifuges, cell sorters, separators and mixers, etc. [12, 14, 28, 35, 42].

The results obtained showed that the flow pattern at the microcavity entrance is the key for the mass transfer into the cavity [40] and that velocity decreases with the distance from microcavity entrance [41]. This allowed to construct many microdevices, in which microvortices in microcavity play a key role for its operations, for instance cell sorter, equipment for cultivation of cells [28, 32], etc. Similarly, explanation of the phenomena occurring in long open type nanocavity seems to be essential for construction of many nanodevices in which flow in nanochannels with nanocavities occurs. The investigation of fluid flow inside a long open type nanocavities helps to gain understanding of many complex phenomena and the nature of numerous biological and physical processes [8, 23]. In contrast to the relatively well studied flows in microcavities, described in numerous papers [7, 30, 33, 40, 41], in literature there is very little information available on flows in nanocavities [3, 6, 10, 19]. The potential use of nanovortices in nanosystems seems to be very large, for example in sorting particles, for DNA manipulation, for which, presently, wide nanocavities have some applications [29, 31].

The flow in nanocavities is difficult to study due to its nanometre size flow domain. In this scale, molecular interactions between fluid and nanochannel wall have impact on the fluid flow structure [5, 21, 22, 26, 38], so one can expect that a cavity width and wall material will have effect on flow pattern inside nanocavity. While microvortex study was possible using experiment or Navier-Stokes predictions, in case of nanovortex, the problem can be treated only by an atomistic method as well as other problems of nanomechanics [15, 41], because for this geometric scale of the phenomenon, continuum mechanics methods are inapplicable to handle it [15]. Experimental investigations in this scale are difficult to perform as well as limited and very often impossible to perform. For this reason, research is conducted using molecular dynamics method.

Shear-driven nanocavity flow was studied using MD by Greenspan [10]. The results have been commented in reference [3]. Chen et al. investigated 2D lid driven cavity flows in three cavity shapes, rectangular, half-circular and beer bucket with the MD method, and showed that nanocavity geometry affects nanovortex strength. All papers mentioned above pertain to nanocavities for which value of aspect ratio, which is defined as a quotient of cavity depth to its width, does not exceed 1. Only in [16–20] long, open type nanocavities with aspect ratio greater than 3 were considered. Results indicated that recirculation of flow within the nanocavity appeared.

The effect of nanocavity aspect ratio on nanovortex formation in long open type nanocavity is displayed in [19]. The question how the wall material affects vortex formation was raised in [18]. Results presented in both papers show that after 19 ns of the flow, the strongest vortex is situated near entrance to the nanocavity.

In microchannels, the strength and emergence of vortex structures is strongly correlated with the velocity value of the fluid flow in the main channel which induces the flow in cavity [37].

Since in [19] the threshold value of the force enforcing the flow of water in the main nanochannel which induces nanov-

\*e-mail: a-kordos@prz.edu.pl

Manuscript submitted 2017-11-13, revised 2018-01-15 and 2018-01-31, initially accepted for publication 2018-02-03, published in April 2018.

ortices in nanocavities is given, in the present paper we want to examine whether the main vortex created at the entrance to the nanocavity in such flow conditions is a stable structure. We focus on investigation of main vortex evolution in first 18 ns of the water flow. For this purpose, we analyse changes in the velocity field at entrance to nanocavity every 1 ns of the flow. We study water flows in the 25.2 nm long open type rectangular cavity of 3.6 aspect ratio for quartz wall materials limiting the flow. Molecular dynamics simulation is applied to investigate the time development of nanovortex motion in the upper part of a long, 2D open type nanocavity, situated perpendicularly to the nanochannel (Fig. 1), where the Poiseuille water flow occurs.

Nanocavity entrance is crucial for mass transfer and is not recognized yet. The fluid circulation zone has to be investigated in detail, because findings have strong potential for application in nano-bio-devices.

In MD simulation, the computer representations of real materials: water and hydroxylated alpha-quartz are used. The simulation was performed by LAMMPS [24] program. The simulation corresponds to the 18 ns of real water flow. To visualize the nanovortex formation, a sequence of images of water velocity vector fields in the nanocavity was plotted using MD simula-

tion data. The average velocity vector fields were obtained by averaging MD data with the bin method [32, 36]. Averaging data from MD simulation at equal time intervals of the flow allowed to plot images of the averaged vector velocity fields at these intervals. The obtained sequence of images representing vector velocity distributions at successive time intervals, shows the nanovortex evolution depicting the formation mechanism.

Results obtained in the paper give new insight into main nanovortex structure in nanocavities:

- they demonstrate that the nanovortex at the entrance to the nanocavity of aspect ratio 3.6 remains a stable structure if maximum water velocity in the main channel which induces the flow in nanocavity is equal to  $V^* = 3.6 * 10^{-2}$ ;
- they show that the shape and position of the nanovortex centre vary over the time of 18 nanoseconds.

To our knowledge the evolution of nanovortex in quartz nanocavity has not been studied yet, so presented research is the first.

## 2. Molecular dynamics simulation details

The flow system consists of water confined in between two parallel quartz walls with the long, rectangular nanocavity, situated perpendicular to the lower wall. It is identical as in [18, 19] and shown in Fig. 1. The dimensions of the MD simulation unit cell in the  $x, y, z$  directions are  $L_x = 21$  nm,  $L_y = 57.2$  nm and  $L_z = 7.9$  nm respectively. The periodic boundary conditions are used in coplanar directions  $x$  and  $z$ . Details on the numbers of molecules used in simulations and dimensions of the computational domain are presented in Table 1. To model the upper channel wall 7740 single alpha-quartz crystal cells are used, whereas to model the lower wall 27576. Details on construction of the nanocavity in the MD unit cell can be found in [19].

Table 1  
MD unit cells dimensions

$L_x$ [nm]	$L_y$ [nm]	$L_z$ [nm]	$w$ [nm]	$l$ [nm]	$L$ [nm]	Total number of atoms
21	57.2	7.9	7	25.2	47.2	782836

The water is modelled by TIP4P/2005 molecular water model [1], the hydroxylated alpha-quartz by ClayFF [9] potential. In TIP4P/2005 model interaction potential is represented as a sum of Coulombic (1) and Lennard-Jones (L-J) (2) potentials, and only oxygen atoms interact via Lennard-Jones potentials (2) with constants  $\epsilon_f = 0.7749 * 10^{-21}$  kJ/mol,  $\sigma_f = 3.1589 * 10^{-10}$  m. Charged sites in this model are situated on two hydrogen atoms ( $q = 0.5564e$ ) and a massless site ( $q = -1.1128e$ ).

$$U_C = \frac{1}{4\pi\epsilon_0} \sum_{i \neq j} \frac{q_i q_j}{r_{i,j}} \quad (1)$$

where  $\epsilon_0$  – dielectric constant,  $r_{i,j}$  denotes distance between atoms  $i$  and  $j$ .

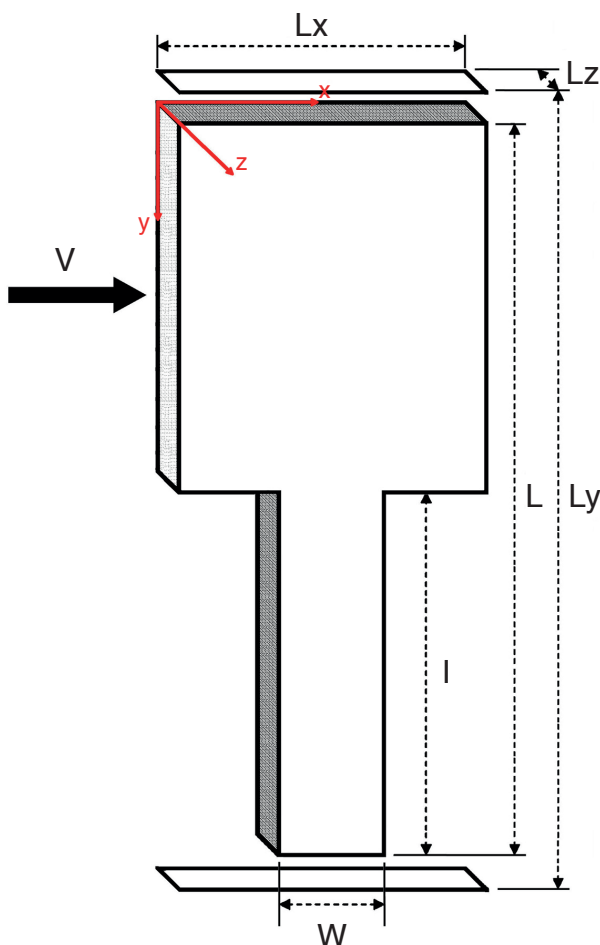


Fig. 1. Sketch of the geometry of the nanocavity

Table 2  
Parameters values of potential (1) and (2) for quartz ClayFF model  
(from [9])

Atom type	$\sigma_w * 10^{-10}$ [m]	$\varepsilon_w$ [kJ/mol]	$q$ [e]
Si	3.30203	$7.7 * 10^{-6}$	2.1
O	3.16556	0.65017	-1.05
H	0	0	0.425
O (in group -OH)	3.16556	0.65017	-0.95

$$U_{LJ} = 4\varepsilon \sum_{i \neq j} \left[ \left( \frac{\sigma}{r_{i,j}} \right)^{12} - \left( \frac{\sigma}{r_{i,j}} \right)^6 \right]. \quad (2)$$

ClayFF potential [9] of the hydroxylated alpha-quartz is represented as the sum of bonded valence interactions (stretching and angular) which are given by (3), (4) respectively, and non-bonded described by Coulombic (1) and Lennard-Jones potential. Values of parameters  $\sigma_w$ ,  $\varepsilon_w$  and  $q$  of (1) (2) are listed in Table 2.

$$U_{bond} = \sum k_{i,bond} (r_i - r_0)^2 \quad (3)$$

and

$$U_{angle} = \sum k_{i,j,angle} (\theta_{i,j} - \theta_0)^2 \quad (4)$$

where  $k_{i,bond} = 2319 \text{ kJ/mol } \text{\AA}^2$  is the bond spring constant,  $r_i$  is the bond distance, and  $r_0$  is the equilibrium bond distance, analogically  $k_{i,j,angle}$  is the bonding force constant,  $\theta_{i,j} = 126 \text{ kJ/mol rad}^2$  is the instantaneous bond angle, and  $\theta_0$  is the equilibrium bond angle.

The water-quartz interaction is calculated by the Coulombic potential and Lennard-Jones potential, where the Lorentz-Berthelot rule is used to calculate the values of L-J parameters. The cutoff distance for van der Waals and electrostatic interactions was set to 1.0 nm [15].

Water density was  $\rho^* = 1.05$  ( $\rho^* = \rho \sigma_f^3$ ,  $\rho = 997 \text{ kg/m}^3$ ), for quartz the value of the density was  $\rho^* = 2.79$  ( $\rho = 2650 \text{ kg/m}^3$ ). The initial velocities of the quartz and water molecules follow from the Maxwell-Boltzmann distribution and correspond to the temperature  $T^* = 3.22$  ( $T = 300 \text{ K}$ ,  $T^* = T k/\varepsilon$ , where  $k$  is Boltzmann's constant). To control the temperature of the system Nosé-Hoover thermostat [2] [4] is applied. Following an initial equilibration phase (100,000 time steps), the temperature of the system was set to  $T^* = 3.22$ .

To develop a Poiseuille flow, we applied a force equal to  $F_{ext}^* = 6.8 * 10^{-3}$  ( $F_{ext}^* = F_{ext} \sigma_f / \varepsilon$ ) in  $x$  direction on the mass centre of every water molecule situated in nanochannel, as in [19], which caused maximum water velocity in the nanochannel  $V_M^* = 3.6 * 10^{-2}$ . The time step for simulation:  $\tau^* = 6.58 * 10^{-4}$  ( $\tau^* = \sigma_f^{-1} (m/\varepsilon)^{-1/2} t$ ,  $t = 1 * 10^{-15} \text{ s}$ ); constant values  $\sigma_f = 3.1589 * 10^{-10} \text{ m}$ ,  $\varepsilon_f = 0.7749 \text{ kJ/mol}$  – for TIP4P/2005 water model [1]). For the simulations we used LAMMPS mo-

lecular dynamics simulator [24]. All data used for calculations is taken after equilibration, every 50 time steps (t.s.) (50 fs) data is collected. Performed simulation (18,000,000 t.s.) corresponds to 18 ns of real water flow.

### 3. Results and discussion

Findings on flow in nanocavities [18–20] confirm that the largest circulation has a main vortex near the entrance to the nanocavity (Fig. 6 and Fig. 12 in [19]). Because of that in the present work we focus on study of time development of the flow field in the upper part of the nanocavity. The flow field under investigation is marked with blue frame in Fig. 2 and denoted as U. The dimension of U domain in  $x$  and  $y$  directions is equal 7 nm and 5.5 nm.

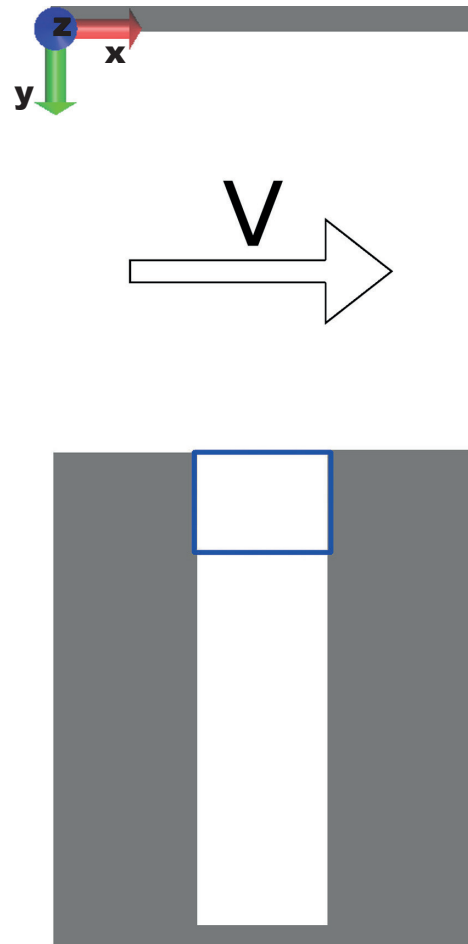
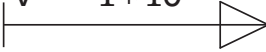


Fig. 2. Geometry of the flow field with U domain (marked by blue frame)

To visualize main nanovortex formation, a sequence of images of water velocity vector  $V^*$  in the U domain was plotted and is presented in Fig. 3. Every plot represents water velocity vector field received at 1 ns interval.

$$V^* = 1 * 10^{-2}$$


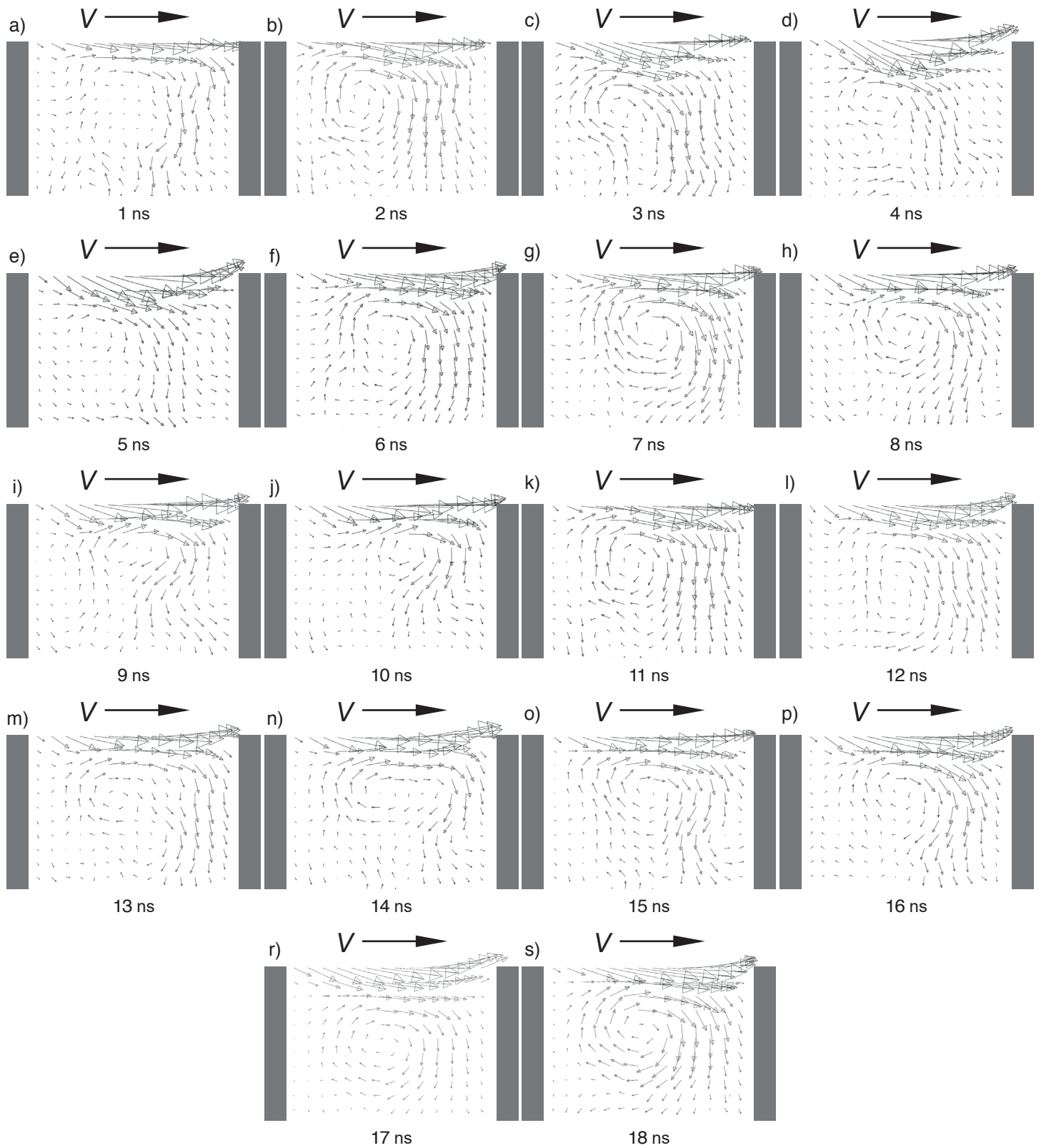


Fig. 3. Sequence of eighteen views of the velocity vector field in the upper part of the nanocavity (U domain), obtained at intervals of 1 nano-second. The view at: a) – 1 ns, b) – 2 ns, c) – 3 ns, d) – 4 ns, e) – 5 ns, f) – 6 ns, g) – 7 ns, h) – 8 ns, i) – 9 ns, j) – 10 ns, k) – 11 ns, l) – 12 ns, m) – 13 ns, n) – 14 ns, o) – 15 ns, p) – 16 ns, r) – 17 ns, s) – 18 ns

Microscopic properties were obtained by sampling and averaging a large number of MD simulation data. To plot the velocity vector fields, the elementary MD cell was divided into 3600 bins of dimensions  $0.5 \text{ nm} \times 0.5 \text{ nm} \times L_z$ . It was obtained by dividing the MD volume into 40 parts in  $x$  direction and 90 parts in  $z$  direction. In every bin  $B_{nm}$ , the average value of water velocity components (in  $x$  and  $z$  directions) was calculated with the CAM (cumulative average measurement) method [36].

Averaging data from molecular dynamics simulation at equal time intervals of the flow, each equal to 1,000,000 t.s. (which corresponds to 1 ns of real flow) allowed to plot images of the averaged velocity vector fields at these intervals. The obtained sequence of 18 images (Fig. 3) representing velocity vector distributions at successive time intervals, shows the main nanovortex evolution depicting the formation mechanism in first 18 ns of the real water flow. Sizes of velocity vectors correspond to the velocity magnitude.

Because of the chaotic nature of the molecular collisions, high value of thermal velocity, and also because of the fact that the simulation is performed with a limited number of molecules, the values of computed macroscopic quantities fluctuate about their averages with some statistical errors.

The results obtained show that the water flow picture changes every nanosecond, the dominant structure is the main vortex, position and size of which change in time. Initial analysis of presented results allows us to say, that main nanovortex evolution process seems to be divided into three phases: initial (I), formation (II) and stabilisation (III).

**3.1. Initial phase.** The initial phase corresponds to the first nanosecond of the flow. Flow structures in U regime (Fig. 3a) are not yet clearly visible, the main nanovortex starts to form.

**3.2. Formation.** The second phase concerns the formation and evolution of main nanovortex. It starts from the second nano-

second of the flow (Fig. 3b) and finishes at 14 ns (Fig. 3o). In this phase we can observe that sequential stages - nanovortex structures appearing periodically at 6 ns of the flow (Fig. 3b–g) correspond to Fig. 3h–l (5 ns of the flow) and Fig. 3m–p (4 ns of the flow).

At 2 ns of the flow (Fig. 3b) the nanovortex structure forms. At 3 ns (Fig. 3c), the main nanovortex grows, moves down and its structure acquires a more elliptical silhouette. At 4 ns (Fig. 3d), the nanovortex structure starts to vanish, passing energy to the bottom of the cavity. Within the next 3 ns (5–7 ns, Fig. 3e–g), the main nanovortex structure becomes clearly defined, and acquires more round silhouette.

Between 8 ns and 12 ns of the flow (Fig. 3h–l) we can observe evolution of the main nanovortex structure similar to those in the first 7 nanoseconds. Analogically, we can find similarities in nanovortex structure between 13 ns and 16 ns (Fig. 3m–p).

**3.3. Phase III.** Starts at 16 ns of the flow (Fig. 3p–s). The main nanovortex seems to be fully formed and reaches its final shape. From 17 ns (Fig. 3r) its localization stabilizes, and subsequent changes occur indeed at “frozen” flow structure. The nanovortex is formed near the entrance part to the nanocavity and its centre is located at  $y/l = 0.1$ ,  $x/w = 0.44$  (Fig. 4). The centre is shifted left from the nanocavity axis and its distance from the nanocavity lid is equal to 2.52 nm.

## 4. Conclusions

The purpose of performed research was to investigate water nanovortex evolution in 2D open type long nanocavity with aspect ratio equal to 3.6.

We have presented new results based on non-equilibrium molecular dynamics simulations of water flow inside the open

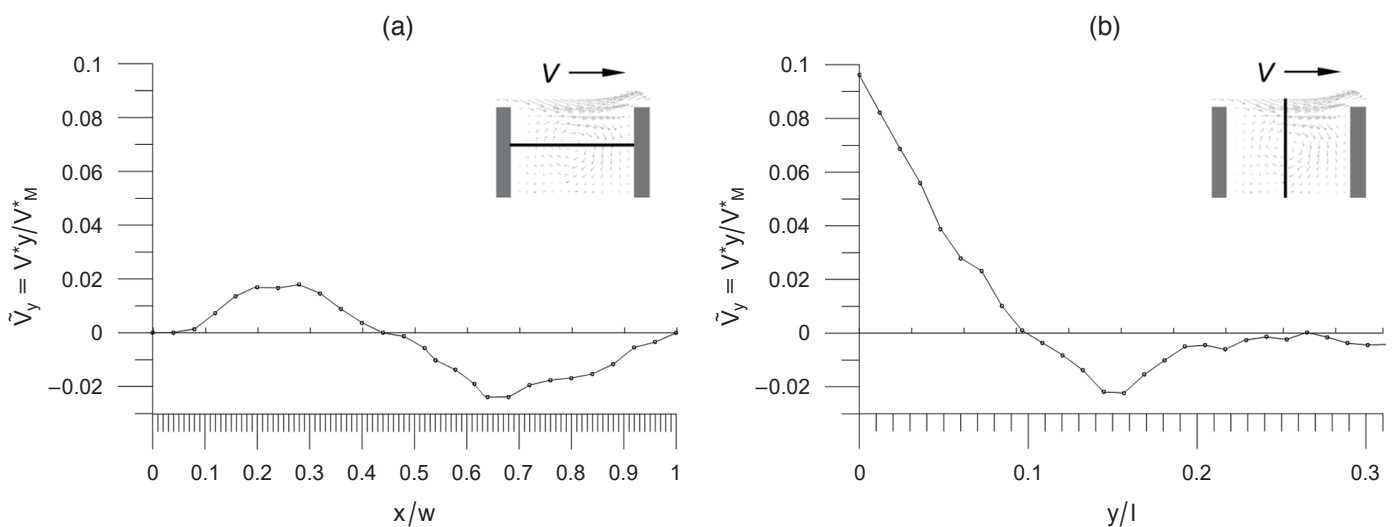


Fig. 4. Normalized water velocity components: a)  $\tilde{V}_y = V_y^*/V_M^*$  distributions in planes crossing the nanovortex centre after 18 ns of the flow, b)  $\tilde{V}_x = V_x^*/V_M^*$  distributions in planes crossing the nanovortex centre after 18 ns of the flow. Dots denote calculated values, lines have been added to highlight value changes

type long nanocavity of 25.2 nm depth, 7 nm width, perpendicular to the main channel, where Poiseuille flow occurs. The water flow in the nanocavity was induced by the flow in the main channel. To visualize the nanovortex formation, a sequence of images of water velocity vector fields in the nanocavity was plotted using MD simulation data. The average velocity vector fields were obtained by averaging MD data with the CAM method [36]. Averaging data from MD simulation at equal time intervals of the flow allowed for plotting images of the averaged vector velocity fields at these intervals. The obtained sequence of images, representing vector velocity distribution at successive time intervals, show the nanovortex evolution depicting the formation mechanism in first 18,000,000 t.s. of performed simulation, which corresponds to the first 18 ns of real water flow.

The findings indicate that although the shape and position of the nanovortex centre vary over time, it remains a stable structure in the flow field at the entrance to the nanocavity.

Results show that nanovortex evolution in nanocavity is a complex process, and this area needs further investigations, because it is crucial for effective design of the bio-nano-devices.

We hope that in the future the experiment or further MD studies on dynamics of nanovortices in nanocavities by MD will allow for a study of nanovortex evolution in nanocavity in a longer period of time than the one presented in this manuscript.

**Acknowledgement** to ICM Warsaw University for the access to high power computers (Research Project No. G45–8).

## REFERENCES

- [1] J.L.F. Abascal and C. Vega, “A general purpose model for the condensed phases of water: TIP4P/2005”, *Journal of Chemical Physics* 123(23), 234505 (2005).
- [2] M.P. Allen and D.J. Tildeslaey: *Computer simulation of Liquids*, Clarendon press, Oxford, 1991.
- [3] W.T. Ashurst, “Comments on Molecular cavity flow by Donald Greenspan”, *Fluid Dynamics Research* 29(3), 221–223 (2001).
- [4] C. Braga and K.P. Travis, “A configurational temperature Nose-Hoover thermostat”, *Journal of Chemical Physics* 123(13), 134101 (2005).
- [5] M. Cieplak, J. Koplik, and J.R. Banavar, “Molecular dynamics of ows in the Knudsen regime”, *Physica A* 287(1–2), 153–160 (2000).
- [6] C.K. Chen and D.T.W. Lin, “TIP4P potential for lid-driven cavity flow”, *Acta Mechanica* 178(3–4), 223–237 (2005).
- [7] M. Cheng and K.C. Hung, “Vortex structure of steady flow in a rectangular cavity”, *Computers and Fluids* 35(10), 1046–1062 (2006).
- [8] M.W. Collins and C.S. Koenig: *Micro and Nano Flow Systems for Bioanalysis*, Springer, New York, 2013
- [9] T.R. Cygan, J.J. Liang, and A.G. Kaliniche, “Molecular Models of Hydroxide, Oxyhydroxide, and Clay Phases and the Development of a General Force Field”, *Journal of Physical Chemistry B* 108(4), 1255–1266 (2004).
- [10] D. Greenspan, “The extraction of laminar flow from certain Brownian motions”, *Computers and Mathematics with Applications* 48(12), 1915–1928 (2004).
- [11] T.A. Halgren, “The representation of van der Waals (vdW) interactions in molecular mechanics force fields: potential form, combination rules, and vdW parameters”, *Journal of the American Chemical Society* 114(20), 7827–7843 (1992).
- [12] A. Haller, A. Spittler, L. Brandhoff, H. Zirath, D. Puchberger-Enengl, F. Keplinger, and M.J. Vellekoop, “Microfluidic Vortex Enhancement for on-Chip Sample Preparation”, *Micro-machines* 6(2), 239–251 (2015).
- [13] W. Humphrey, A. Dalke, and K. Schulten, “VMD – Visual Molecular Dynamics”, *Journal of Molecular Graphics* 14(1), 33–38 (1996).
- [14] S.C. Hur, A.J. Mach, and D. Di Carlo, “High-throughput size-based rare cell enrichment using microscale vortices”, *Biomicrofluidics* 2011b(5), 022206 (2011).
- [15] G. Karniadakis, A. Beskok, and N. Aluru: *Microflows and Nanoflows. Fundamentals and Simulation*, Springer-Verlag, New York, 2005.
- [16] A. Kordos and A. Kucaba-Pietal, “Computer simulation of nanoflows in chromatography columns”, *Proceedings of the 35th IC ITI; ISBN 978–953–7138–31–8*, (2013).
- [17] A. Kordos: *Modeling of hydrodynamics and mass transport in chromatographic columns using molecular dynamics simulation*, PhD thesis, Rzeszow University of Technology, 2015.
- [18] A. Kordos and A. Kucaba-Pietal, “Effect of wall material on water nanovortices formation in 2D long open type nanocavity. Molecular Dynamics study.”, *Journal of Molecular Liquids*, 251, 480–486 (2018)
- [19] A. Kucaba-Pietal and A. Kordos, “Water nanovortices formation in 2D open type long nanocavities. Molecular dynamics study.”, *Journal of Molecular Liquids*, 249, 160–168 (2018)
- [20] A. Kucaba-Pietal and A. Kordos, “Molecular Dynamic simulation of water flows in nanochannels with nanocavities. Vortices formation”, *Proceedings of XXII Fluid Mechanics Conference, 11–14. 09.2016, Slok/ Belchatow* (2016).
- [21] A. Kucaba-Pietal, Z. Walenta, and Z. Peradzynski, “Molecular dynamics computer simulation of water flows in nanochannels”, *Bull. Pol. Ac.: Tech.* 57(1), 55–56 (2009).
- [22] A. Kucaba-Pietal, Z.A. Walenta, and Z. Peradzynski, “Water flows in copper and quartz nanochannels”, *Mechanics of the 21th Century*, Springer, Dordrecht, 2005.
- [23] K.K. Jain: *The Handbook of Nanomedicine*, Springer, New York, 2012
- [24] LAMMPS, Sandia National Laboratories, <http://lammps.sandia.gov/>
- [25] T.M. Liou and C.T. Lin, “Three-dimensional rarefied gas flows in constricted microchannels with different aspect ratios: asymmetry bifurcations and secondary flows”, *Microfluidics and Nanofluidics* 18(2), 279–292 (2015).
- [26] C. Liu and Z. Li, “Flow regimes and parameter dependence in nanochannel flows”, *Physical Review E* 80(3), 036302 (2009).
- [27] A.J. Mach, J.H. Kim, A. Arshi, S.C. Hur, and D. Di Carlo, “Automated cellular sample preparation using a Centrifuge-on-a-Chip.”, *Lab Chip* 11(17), 2827–2834 (2011).
- [28] J. Marchalot, Y. Fouillet, and J.L. Achard, “Multi-step microfluidic system for blood plasma separation: Architecture and separation efficiency.”, *Microfluidics and Nanofluidics* 17(1), 167–180 (2014).
- [29] M.B. Mikkelsen, W. Reisner, H. Flyvbjerg, and A. Kristensen, “Pressure-Driven DNA in Nanogroove Arrays: Complex Dynamics Leads to Length- and Topology-Dependent Separation”, *Nano Letters* 11(4), 1598–1602 (2011)

- [30] N. Osterman, J. Derganc, and D. Svensek, "Formation of vortices in long microcavities at low Reynolds number", *Microfluidics and Nanofluidics* 20(2), 33 (2016).
- [31] W. Reisnera, N.B. Larsend, H. Flyvbjergb, J.O. Tegenfeldtc, and A. Kristensenb, "Directed self-organization of single DNA molecules in a nanoslit via embedded nanopit arrays", *Proceedings of the National Academy of Sciences* 106(1), 79–84 (2009)
- [32] P. Sajeesh and A.K. Sen, "Particle separation and sorting in microfluidic devices: A Review", *Microfluidics and Nanofluidics* 17(1), 1–52 (2014).
- [33] F. Shen, P. Xiao, and Z. Liu, "Microparticle image velocimetry (mPIV) study of microcavity flow at low Reynolds number.", *Microfluidics and Nanofluidics* 15(5), 1 (2015).
- [34] A.A. Skelton, P. Fenter, J.D. Kubicki, D.J. Wesolowski, and P.T. Cummings, "Simulations of the Quartz(1011)/Water Interface: A Comparison of Classical Force Fields, Ab Initio Molecular Dynamics, and X-ray Reflectivity Experiments", *The Journal of Physical Chemistry C* 115(5), 2076–2088 (2011).
- [35] E. Sollier, M. Cubizolles, Y. Fouillet, and J.L. Achard, "Fast and continuous plasma extraction from whole human blood based on expanding cell-free layer devices.", *Biomedical Microdevices* 12(3), 485–497 (2010).
- [36] M.W. Tysanner and A.L. Garcia, "Non-equilibrium behavior of equilibrium reservoirs in molecular simulations, International Journal of Numerical Methods in Fluids", *International Journal for Numerical Methods in Fluids* 2050, 1–12 (2005).
- [37] E.M. Wahba, "On the steady flow in a rectangular cavity at large Reynolds numbers: A numerical and analytical study", *European Journal of Mechanics B/Fluids* 44, 69–81 (2014).
- [38] Z.A. Walenta, A. Kucaba-Pietal, and Z. Peradzynski, "Fluid flows in narrow channels", *Journal Technical Physics* 1, 65–70 (2009).
- [39] Z.A. Walenta and A.M. Slowicka, "Structure of Shock Waves in Dense Gases and Liquids – Molecular Dynamics Simulation", 20th International Shock Interaction Symposium, 20–24 August 2012, Book of Proceedings, KTH Stockholm, Sweden, 215–218, (2012).
- [40] A.G. Yew, D. Pinero, A.H. Hsieh, and J. Atencia, "Low Peclet number mass and momentum transport in microcavities", *Applied Physics Letters* 102(8), 084108 (2013).
- [41] Z.T.F. Yu, Y.K. Lee, M. Wong, and Y. Zohar, "Fluid flows in microchannels with cavities", *Journal of Microelectromechanical Systems* 14(6), 1386–1398 (2005).
- [42] J. Zhou, S. Kasper, and I. Papautsky, "Enhanced size dependent trapping of particles using microvortices", *Microfluidics and Nanofluidics* 15(5), 611–623 (2013).